Field cancellation by a two-level atom in a multimode cavity driven by a time-dependent field

D. A. Cardimona and Karl Koch
Air Force Phillips Laboratory, 3550 Aberdeen Avenue, S.E., Kirtland Air Force Base, New Mexico 87117

P. M. Alsing
High Performance Computing Education and Research Center, University of New Mexico, 1601 Central Avenue, N.E., Albuquerque, New Mexico 87131

(Received 14 June 1996; revised manuscript received 13 September 1996)

We investigate the behavior of a two-level atom in a multimode cavity driven from the side by a time-dependent field. The time-dependent fields we have looked at are (i) pure amplitude modulated, (ii) pure frequency modulated, (iii) single sideband, and (iv) general three-mode fields. Each of these fields results in two (for the single-sideband case) or three modes separated by the modulation frequency. We find that when the driving field mode spacing is a multiple of the cavity mode spacing, the multimode cavity field created by the driven two-level atom becomes exactly 180° out of phase with the external driving field in steady state. This results in a zero net field at the position of the atom and, hence, the atom remains unexcited regardless of the strength of the external driving field. This is very reminiscent of the field-induced transparency effect as described by Cardimona *et al.* [J. Phys. B **15**, 55 (1982)] in which the various dipole transitions of a multilevel atom dressed by a coherent field are driven 180° out of phase with each other, producing a zero net fluorescence. We also show that, in the limit of an infinite cavity, the multimode equations reduce to the neoclassical equations of Stroud and Jaynes [Phys. Rev. A **1**, 106 (1970)]. [S1050-2947(97)07701-9]

PACS number(s): 42.50.Dv, 42.50.Hz

I. INTRODUCTION

A wealth of knowledge and intuition has been gained from the study of the idealized system of a two-level atom coupled to a single-mode field [1]. The slightly more complicated models of a three-level atom or a two-level atom in a cavity or interactions with a multimode field are natural progressions in understanding the complex interaction of light and matter under more physical constraints. The radiative properties of atoms inside a cavity have been the subject of intense investigations in recent years under the broad heading of cavity quantum electrodynamics. Some of the more exotic effects uncovered in theoretical work dealing with a single atom in a cavity should become more accessible in the laboratory once the technologies of atomic cooling and trapping are incorporated into experiments [2]. One model system that has received a lot of theoretical attention comprises a single atom coupled strongly to a single quantized cavity mode, driven by an external coherent field, and including cavity damping and spontaneous emission. By allowing for a flux of energy through the atom-cavity system, the dynamics can evolve to a nonequilibrium steady state that exhibits many interesting and novel features [3–8].

In this work we explore a modified version of this model in an idealized limit. We drive the atom directly with a two- or three-mode external coherent field and examine the situation of perfectly reflecting cavity mirrors (lossless cavity). We will also provide a brief glimpse at the effect of including loss out of the cavity. The driving field will be created using three modes of varying amplitude and phase, separated by a fixed frequency spacing. We will look at driving fields created via pure amplitude modulation (AM), which result in sidebands that are in phase with the central mode, and fields created via pure frequency modulation (FM), which result in sidebands that are in quadrature with the central mode. We will also look at single-sideband driving fields and arbitrary-intensity double-sideband fields, created via combinations of AM and FM. Because of the multimode nature of these modulated driving fields, we will allow the cavity to support more than one quantized mode. We analyze the effect on the atomic fluorescence when the allowed cavity modes are varied in number and in frequency separation.

A novel feature arises in steady state when the modulation amplitude of the external driving field is zero. Even though a coherent field exists within the cavity in steady state, maintained by the perfectly reflecting mirrors, the atom decouples from this field, and the fluorescence turns off (see Ref. [9]). For highly reflecting, but not perfect, mirrors, the fluorescence is strongly suppressed. This decoupling of the atom from the field is exactly analogous to the atomic decoupling leading to the three-level field-induced transparency described by Cardimona *et al.* [10–12], and later modified by Harris and co-workers [13,14]. (Harris's version of electromagnetically induced transparency has been observed experimentally in atoms [15].) In the following work we find that even when the driving field is modulated, the decoupling takes place whenever the cavity field mode spacing is a harmonic of the driving field mode spacing.

II. REVIEW OF SINGLE-MODE-FIELD RESULTS

We will first review the results obtained when a single-mode field is incident from the side of a single-mode cavity containing a single two-level atom (see Fig. 1). With this in mind, the wave equation is

$$\left(\frac{\partial^2}{\partial t^2}-c^2\frac{\partial^2}{\partial z^2}+4\pi\sigma\frac{\partial}{\partial t}\right)E(z,t)=-4\pi\frac{\partial^2}{\partial t^2}P(z,t), \quad (1)$$

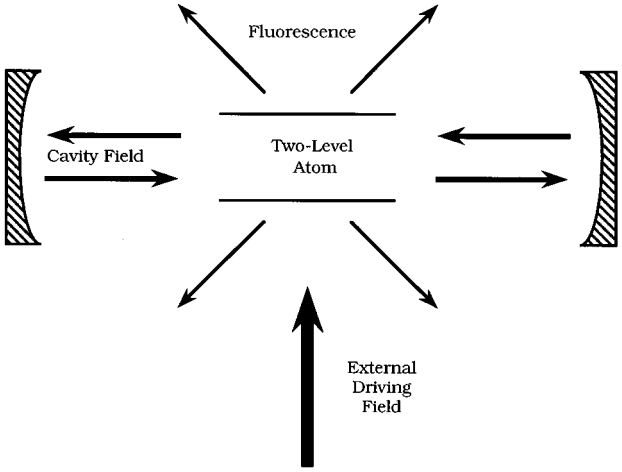

FIG. 1. The externally driven two-level atom-in-a-cavity system under consideration in this paper.

where the σ term comes from the $J=\sigma E$ constitutive relation and will account phenomenologically for the cavity losses. Defining slowly varying envelopes through the relations

$$E(z,t)=\mathcal{E}(t)\exp[i(\omega t-kz)]+\text{c.c.}, \tag{2a}$$

$$P(z,t)=\mathcal{P}(t)\exp[i(\omega t-kz)]+\text{c.c.}, \tag{2b}$$

we can derive the equation satisfied by the electric fields in the slowly varying envelope approximation (SVEA) as

$$\left(\frac{\partial}{\partial t}+\gamma_c\right)\Omega(t)=-i\,\frac{\alpha c}{T_2}\,r_{12}(t), \tag{3}$$

where we have made the following definitions and substitutions:

$$\Omega(t)\equiv 2d\mathcal{E}(t)/\hbar, \tag{4a}$$

$$\mathcal{P}(t)=\mathcal{N}d^{*}r_{12}(t), \tag{4b}$$

$$\gamma_c\equiv 2\pi\sigma, \tag{4c}$$

$$\alpha\equiv 4\pi\omega\mathcal{N}|d|^2T_2/c\hbar. \tag{4d}$$

Here d is the transition dipole moment, $\mathcal{N}$ is the atomic number density, $r_{12}(t)$ is the slowly varying part of the off-diagonal density matrix element, α is the inverse Beer's absorption length, and T_2 is the dipole dephasing time. Now defining the Bloch variables as $u=r_{12}+r_{21}$, $iv=r_{12}-r_{21}$, and $w=r_{22}-r_{11}$, and writing the Rabi frequency in real and imaginary parts as $\Omega=(\Omega'+\chi)+i\Omega''$, where χ is the constant monochromatic field applied to the side of the cavity and $\Omega'+i\Omega''$ is the cavity field, we may write the Maxwell-Bloch equations for the atom-cavity system as

$$\dot{u}=-u/T_2-\Delta v-\Omega''w, \tag{5a}$$

$$\dot{v}=-v/T_2+\Delta u+(\Omega'+\chi)w, \tag{5b}$$

$$\dot{w}=-(w-w_{\text{eq}})/T_1-(\Omega'+\chi)v+\Omega''u, \tag{5c}$$

$$\dot{\Omega}'+\gamma_c\Omega'=\frac{\alpha c}{2T_2}\,v, \tag{5d}$$

$$\dot{\Omega}''+\gamma_c\Omega''=-\frac{\alpha c}{2T_2}\,u, \tag{5e}$$

where T_1 is the population decay time, $\Delta=\omega_{21}-\omega$ with ω_{21} the atomic transition frequency, and w_{eq} is the equilibrium population inversion.

From these equations we find the steady-state values to be

$$u_{\text{ss}}=\frac{[(\Omega'_{\text{ss}}+\chi)\Delta T_2-\Omega''_{\text{ss}}]w_{\text{eq}}T_2}{1+(\Delta T_2)^2+[(\Omega'_{\text{ss}}+\chi)^2+(\Omega''_{\text{ss}})^2]T_1T_2} \tag{6a}$$

$$=-\Omega''_{\text{ss}}T_2\,\frac{2\gamma_c}{\alpha c}, \tag{6b}$$

$$v_{\text{ss}}=\frac{[(\Omega'_{\text{ss}}+\chi)+\Omega''_{\text{ss}}\Delta T_2]w_{\text{eq}}T_2}{1+(\Delta T_2)^2+[(\Omega'_{\text{ss}}+\chi)^2+(\Omega''_{\text{ss}})^2]T_1T_2} \tag{6c}$$

$$=\Omega'_{\text{ss}}T_2\,\frac{2\gamma_c}{\alpha c}. \tag{6d}$$

If we have a very good cavity such that $(2\gamma_c/\alpha c)\ll|w_{\text{eq}}|$, we find expressions for the Rabi frequency to first order in $(2\gamma_c/\alpha c w_{\text{eq}})$ to be

$$\Omega'^{(1)}_{\text{ss}}=-\chi\left[1+\left(\frac{2\gamma_c}{\alpha c w_{\text{eq}}}\right)\right], \tag{7a}$$

$$\Omega''^{(1)}_{\text{ss}}=-\chi(\Delta T_2)\left(\frac{2\gamma_c}{\alpha c w_{\text{eq}}}\right). \tag{7b}$$

From these expressions we see that for a perfect cavity ($\gamma_c=0$), the steady-state cavity field is exactly the applied field, only 180° out of phase, resulting in $u_{\text{ss}}=0=v_{\text{ss}}$ and $w_{\text{ss}}=w_{\text{eq}}$. The two fields cancel at the site of the atom and, for $w_{\text{eq}}=-1$, the atom remains in the ground state, even though the applied field is incident on it continuously (see Ref. [9]).

III. MULTIMODE FIELDS

The question now is: Can this cancellation effect persist in the presence of a multimode external driving field? To investigate this, we apply a general three-mode driving field in place of the single-mode field of Sec. II, and allow the cavity field to develop several modes. We will consider there to be an aperture in the cavity to restrict the transverse variation to the lowest-order mode. Then, putting the atom at the center of the cavity we can approximate the wave fronts as plane waves, and consider only longitudinal cavity modes.

In this approximation, we expand the cavity field $E_c(z,t)$ in terms of the cavity mode functions $\mathcal{U}_n(z)$ as

$$E_c(z,t)=\sum_n C_n(t)\mathcal{U}_n(z)+\text{c.c.}, \tag{8}$$

where the cavity mode functions satisfy Helmholtz's equation

$$\left(\frac{\partial^2}{\partial z^2}+k_n^2\right)\mathcal{U}_n=0 \tag{9}$$

with the appropriate boundary conditions, and are normalized over a cavity of length L such that

$$\frac{2}{L}\int_{-L/2}^{L/2}\mathcal{U}_m^*(z)\mathcal{U}_n(z)dz=\delta_{nm}. \tag{10}$$

The mode amplitudes $C_n(t)$ can be written in terms of slowly varying amplitudes $\mathcal{E}_n(t)$ as

$$C_n(t)=\mathcal{E}_n(t)\exp(i\omega t), \tag{11}$$

so that the cavity field can be written as

$$E_c(z,t)=\sum_n \mathcal{E}_n(t)\mathcal{U}_n(z)\exp(i\omega t)+\text{c.c.} \tag{12}$$

Since in this work we are considering a single atom at the center of the cavity, we will confine the polarization to a region small compared to the variation of the cavity modes. We do this by introducing the Gaussian factor $e^{-z^2/a_0^2}/\sqrt{\pi}$ into the atomic polarization (here a_0 is the Bohr radius). If we now approximate this factor with its δ-function limit $[\lim_{a_0\to 0}e^{-z^2/a_0^2}/\sqrt{\pi}a_0=\delta(z)]$, Eqs. (2b) and (4b) become

$$P(z,t)=\mathcal{N}d^*\left[\left(\frac{u+iv}{2}\right)\exp(i\omega t)+\text{c.c.}\right]\delta(z)a_0. \tag{13}$$

We made this δ-function approximation in anticipation of an integration over z. Inserting these expressions into the wave equation (1) gives

$$\begin{aligned}\sum_n\ &[\ddot{\mathcal{E}}_n+2i\omega\dot{\mathcal{E}}_n-\omega^2\mathcal{E}_n+c^2k_n^2\mathcal{E}_n+2\gamma_c(\dot{\mathcal{E}}_n+i\omega\mathcal{E}_n)]\mathcal{U}_n\\ &\times\exp(i\omega t)+\text{c.c.}\\ =&-2\pi\mathcal{N}d^*[\ddot{u}+i\ddot{v}+2i\omega(\dot{u}+i\dot{v})-\omega^2(u+iv)]\\ &\times\delta(z)a_0\ \exp(i\omega t)+\text{c.c.}\end{aligned} \tag{14}$$

After invoking the SVEA, we multiply both sides of this equation by $\mathcal{U}_m^*(z)$ and integrate over the cavity from $-L/2$ to $L/2$ to obtain

$$\begin{aligned}&2i\omega\dot{\mathcal{E}}_n+(c^2k_n^2-\omega^2)\mathcal{E}_n+2i\omega\gamma_c\mathcal{E}_n\\ &\quad=2\pi\omega^2\mathcal{N}d^*\ \frac{2a_0}{L}\mathcal{U}_n^*(0)(u+iv).\end{aligned} \tag{15}$$

We use the following approximation and definitions:

$$\begin{aligned}c^2k_n^2-\omega^2\equiv\omega_n^2-\omega^2\approx 2\omega(\omega_n-\omega)\equiv 2\omega\Delta_n\equiv 2\omega\ \frac{2\pi n}{\tau_R}\\ \equiv 2\omega n\Delta_c,\end{aligned} \tag{16}$$

where τ_R is the cavity round-trip time and Δ_c is the cavity mode spacing. If we write the Rabi frequency for the nth mode as

$$\Omega_n=\frac{2d}{\hbar}\,\mathcal{E}_n, \tag{17}$$

we find the multimode equivalent of Eq. (3) to be

$$\dot{\Omega}_n+(\gamma_c-i\Delta_n)\Omega_n=-i\ \frac{\alpha c a_0}{T_2 L}\,\mathcal{U}_n^*(0)(u+iv). \tag{18}$$

We will first let $\mathcal{U}_n(0)=1$ and let the cavity support a finite number of modes. Now our general three-mode driving field Rabi frequency can be written as

$$\begin{aligned}\frac{2d}{\hbar}E_{\text{drive}}&=\frac{2d}{\hbar}\{2A\ \cos\omega t+2B\ \cos[(\omega+\delta)t]\\ &\quad+2C\ \cos[(\omega-\delta)t]\}\\ &\equiv\frac{2d}{\hbar}\{2A[1+c_{\text{am}}\cos\delta t]\cos\omega t\\ &\quad-2Ac_{\text{fm}}\sin\delta t\ \sin\omega t\}\\ &\equiv 2\chi'\cos\omega t-2\chi''\sin\omega t=(\chi'+i\chi'')e^{i\omega t}+\text{c.c.}\\ &\equiv\chi e^{i\omega t}+\text{c.c.}\end{aligned} \tag{19}$$

If we assume there is an atomic steady state in which $u_{\text{ss}}=0$, and then search for a solution to Eqs. (5a)–5(c) (now with $\chi\to\chi'$ and a χ'' added to Ω'' everywhere) and Eq. (18), we find

$$\sum_n\ \Omega_n''=-\chi'', \tag{20a}$$

$$v_{\text{ss}}=\left(\sum_n\ \Omega_n'+\chi'\right)w_{\text{ss}}\Big/\ \Gamma, \tag{20b}$$

$$w_{\text{ss}}=-\gamma\Big/\left[\gamma+\left(\sum_n\ \Omega_n'+\chi'\right)^2\Big/\ \Gamma\right], \tag{20c}$$

$$\dot{\Omega}_n''=\Delta_n\Omega_n', \tag{20d}$$

$$\dot{\Omega}_n'=-\Delta_n\Omega_n''+\frac{\alpha c a_0}{T_2 L}\,v_{\text{ss}}, \tag{20e}$$

where $\Gamma=1/T_2$, $\gamma=1/T_1$, $w_{\text{eq}}=-1$, and we have assumed a perfect cavity with $\gamma_c=0$. If we look for conditions in which the atom remains in the ground state in this atomic steady state (taking our cue from the single-mode results in which $w_{\text{ss}}=w_{\text{eq}}=-1$), we find

$$\sum_n\ \Omega_n'=-\chi', \tag{21a}$$

$$v_{\text{ss}}=0, \tag{21b}$$

$$\Omega_n'=A_n\cos(\Delta_n t+\phi_n), \tag{21c}$$

$$\Omega_n''=A_n\sin(\Delta_n t+\phi_n). \tag{21d}$$

Using Eqs. (20a) and (21a), we find that the above steady state is satisfied if

$$\phi_{\pm n}=0, \tag{22a}$$

$$A_0=-\chi_0, \tag{22b}$$

$$A_{\pm n}=-\tfrac{1}{2}\chi_0(c_{\rm am}\pm c_{\rm fm}) \quad \text{for } \Delta_n=\delta, \tag{22c}$$

$$A_{\pm n}=0 \quad \text{for } \Delta_n\neq\delta, \tag{22d}$$

where $\chi_0=(2d/\hbar)A$ from Eq. (19). The various specializations of the general modulated driving field [Eq. (19)] occur in the following manner: (i) $c_{\rm fm}=0\Rightarrow$pure amplitude-modulated field, (ii) $c_{\rm am}=0\Rightarrow$pure frequency-modulated field, and (iii) $c_{\rm am}=c_{\rm fm}\Rightarrow$single-sideband field. These solutions are borne out in the figures of Sec. V.

As pointed out in Ref. [9], the single atom in a cavity interacting with a two-mode field (one driving mode and one cavity mode) is similar to a single field driving an atom having two competing transition paths. In both cases, the competing quantities (the two modes in the atom-in-a-cavity problem and the two transition dipole moments in the three-level-atom problem) develop 180° out of phase with each other. Now we see that, corresponding to Ref. [10], a single atom in a cavity interacting with a multimode field is similar to a single field driving an atom having multiple competing transitions. In the multilevel atom problem, the transition dipole moments become out of phase and quantum mechanically interfere with each other. Here in the present work, the multimode cavity field stabilizes in a 180° out-of-phase configuration when the cavity field mode spacing is a harmonic of the driving field mode spacing ($\Delta_c=\delta/n$), producing a zero net field at the position of the atom.

IV. INFINITE-MODE CAVITY FIELD

In this section we will allow an infinite number of cavity modes by formally integrating the multimode Eq. (18). Doing this we obtain

$$\Omega_n(t)=-i\,\frac{\alpha c a_0}{T_2 L}\,\mathcal{U}_n^*(0)\int_0^t[u(t')+iv(t')]\times\exp[-(\gamma_c-i\Delta_n)(t-t')]dt'. \tag{23}$$

The field that appears in the Bloch equations [Eqs. (5a)–(5c)] is $E_c(z=0,t)$, which is related to

$$\Omega(t)=\sum_{n=-\infty}^{\infty}\Omega_n(t)\mathcal{U}_n(0)=-i\,\frac{\alpha c a_0}{T_2 L}\int_0^t dt'[u(t')+iv(t')]\exp[-\gamma_c(t-t')]\times\sum_{n=-\infty}^{\infty}|\mathcal{U}_n(0)|^2\exp[i\Delta_n(t-t')]. \tag{24}$$

A. Ring cavity

Let us consider the case of a ring cavity. The mode functions for a ring cavity have the property that $|\mathcal{U}_n(z=0)|^2=1$ for all n. Using this property and the Poisson sum formula [16] allows us to simplify the sum within this integral as

$$\begin{aligned}\sum_{n=-\infty}^{\infty}|\mathcal{U}_n(0)|^2\exp[i\Delta_n(t-t')]&=\sum_{n=-\infty}^{\infty}\exp\left[i2\pi n\left(\frac{t-t'}{\tau_R}\right)\right]\\&=\sum_{m=-\infty}^{\infty}\int_{-\infty}^{\infty}dx\,\exp(i2\pi m x)\exp\left[i2\pi x\left(\frac{t-t'}{\tau_R}\right)\right]\\&=\sum_{m=-\infty}^{\infty}\delta\left(m+\frac{t-t'}{\tau_R}\right)=\tau_R\sum_{m=-\infty}^{\infty}\delta(m\tau_R+t-t').\end{aligned} \tag{25}$$

If we recognize that we cannot have a field at a future time interact with the atom in the present, we may now write the cavity field that appears in the Bloch equations 5(a)–5(c) as

$$\Omega(t)=-i\,\frac{\alpha c a_0}{T_2 L}\,\tau_R\sum_{m=0}^{M}[u(t-m\tau_R)+iv(t-m\tau_R)]\times\exp(-\gamma_c m\tau_R). \tag{26}$$

For this ring cavity case, with a round-trip distance of L, we have $\tau_R=L/c$. So we see that the field that interacts with the atom at time t is just that field created at time t plus all of the previous fields that have reflected back to the position of the atom m times (with the maximum of m being the nearest integer less than t/τ_R), with each of these reflected fields being reduced in amplitude due to leakage out of the cavity at the rate of γ_c. In the limit of an infinite cavity length we have

$$\lim_{\tau_R\to\infty}\Omega(t)=-i\,\frac{\alpha a_0}{T_2}[u(t)+iv(t)]. \tag{27}$$

B. Standing-wave cavity

Now let us consider the case of a standing-wave cavity. If the cavity mirrors are taken to be at $z=\pm L/2$, the mode amplitudes satisfy

$$\mathcal{U}_n(z=0)=\sin\left[\frac{\pi n}{L}\,(z+L/2)\right]\Big|_{z=0}=\sin\left(\frac{n\pi}{2}\right), \quad n=1,2,3,\ldots\,. \tag{28}$$

We see that only every other mode contributes, since every other mode in a standing-wave cavity has a mode at the center of the cavity. The sum in Eq. (24) now becomes

$$\frac{1}{2}\sum_{n=-\infty}^{\infty}\exp\left[i2\pi n\left(\frac{t-t'}{\tau_R}\right)\right]\left(1-\frac{e^{in\pi}+e^{-in\pi}}{2}\right), \tag{29}$$

where we have used $\sin^2(n\pi/2)=\frac{1}{2}[1-\cos(n\pi)]$. Using Poisson's sum formula once again allows us to write this as

$$\frac{\tau_R}{2}\sum_{m=-\infty}^{\infty}[\delta(m\tau_R+t-t')-\tfrac{1}{2}\delta(m\tau_R+t-t'+\tau_R/2)-\tfrac{1}{2}\delta(m\tau_R+t-t'-\tau_R/2)]. \tag{30}$$

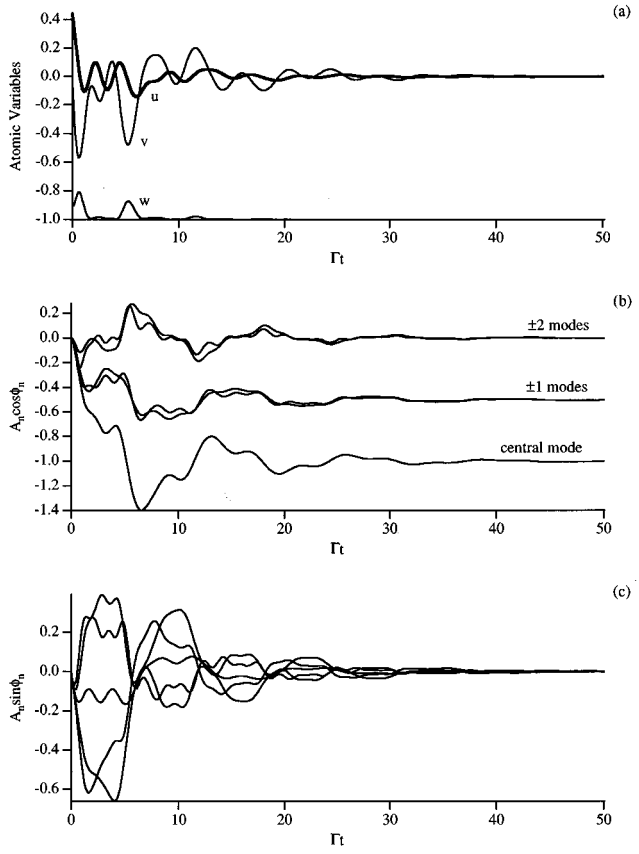

FIG. 2. Five cavity field modes allowed, with $\Delta_c=\delta$. (a) The atomic variables u, v, and w, (b) the real part of the slowly varying cavity field, $A_n\cos\phi_n$, and (c) the imaginary part of the slowly varying cavity field, $A_n\sin\phi_n$, plotted vs Γt.

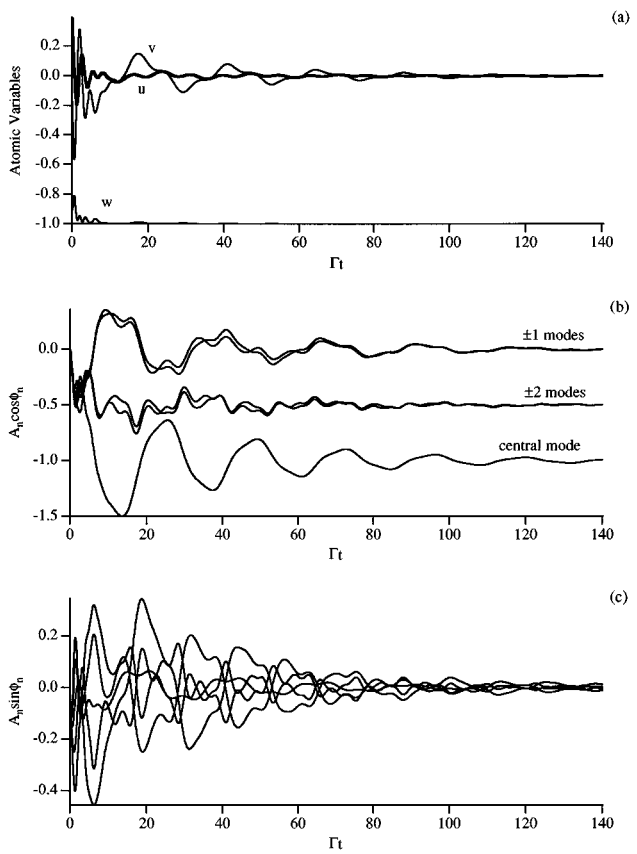

FIG. 3. Five cavity field modes allowed, with $\Delta_c=\delta/2$. (a), (b), and (c) as in Fig. 2.

Now the field appearing in the Bloch equations becomes

$$\begin{aligned}\Omega(t)=&-i\,\frac{\alpha c a_0}{T_2 L}\,\frac{\tau_R}{2}\sum_{m=0}^{M}\exp(-\gamma_c m\tau_R)[p(t-m\tau_R)\\&-\tfrac{1}{2}p(t-m\tau_R+\tau_R/2)\exp(\gamma_c\tau_R/2)\\&-\tfrac{1}{2}p(t-m\tau_R-\tau_R/2)\exp(-\gamma_c\tau_R/2)]\\=&-i\,\frac{\alpha c a_0}{T_2 L}\,\frac{\tau_R}{2}\,p(t)-i\,\frac{\alpha c a_0}{T_2 L}\,\frac{\tau_R}{2}\sum_{m=1}^{M}\{p(t-m\tau_R)\\&\times\exp(-m\tau_R\gamma_c)-p(t-[m-1/2]\tau_R)\\&\times\exp[-(m-1/2)\tau_R\gamma_c]\},\end{aligned}\tag{31}$$

where $p(t)=u(t)+iv(t)$. For this standing-wave cavity case, with a round-trip distance of $2L$, we have $\tau_R=2L/c$. Thus, the field-averaging that occurs in a standing wave (the 1/2 in front) is countered by the doubling of the round-trip time. This field arises from the fact that in a standing-wave cavity, the cavity field interacts with the atom at every half-round-trip time, again escaping from the cavity at the rate of γ_c, as in the ring cavity. Once again in the infinite cavity limit, this cavity field reduces to

$$\lim_{\tau_R\to\infty}\Omega(t)=-i\,\frac{\alpha a_0}{T_2}\,[u(t)+iv(t)].\tag{32}$$

In the infinite cavity limit, the Bloch equations for both types of cavities become

$$\dot{u}=-u/T_2-\Delta v+guw,\tag{33a}$$

$$\dot{v}=-v/T_2+\Delta u+gvw+\chi w,\tag{33b}$$

$$\dot{w}=-(w-w_{\rm eq})/T_1-g(u^2+v^2)-\chi v,\tag{33c}$$

where $g=\alpha a_0/T_2$. These equations are just the neoclassical equations of Stroud and Jaynes [17] where the Lamb shift has been neglected and phenomenological damping has been included. This is not too surprising, since in the infinite-cavity-length limit the atom is sitting in free space and feeling the effects of its own radiation reaction field. If we let g be much greater than both $1/T_2$ and $|\Delta|$, then we can find steady-state solutions to these neoclassical-like equations good to second order in $(1/gw_{\rm eq}T_2)$ and/or $(\Delta/gw_{\rm eq})$,

$$u_{\rm ss}\approx-\frac{\chi}{g}\,\frac{\Delta}{gw_{\rm eq}}\left(1+\frac{2}{gw_{\rm eq}T_2}\right),\tag{34a}$$

$$v_{\rm ss}\approx-\frac{\chi}{g}\left(1+\frac{1}{gw_{\rm eq}T_2}+\frac{1-(\Delta T_2)^2}{(gw_{\rm eq}T_2)^2}\right),\tag{34b}$$

$$w_{\rm ss}\approx w_{\rm eq}\left[1-\frac{\chi^2 T_1}{g}\left(\frac{1}{gw_{\rm eq}T_2}+\frac{1+(\Delta T_2)^2}{(gw_{\rm eq}T_2)^2}\right)\right],\tag{34c}$$

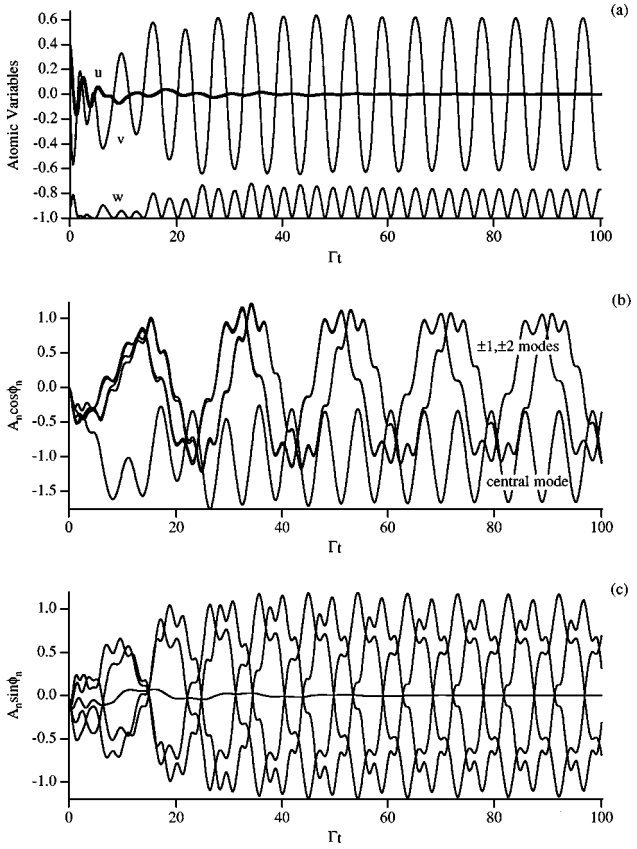

FIG. 4. Five cavity field modes allowed, with $\Delta_c=\delta/1.5$. (a), (b), and (c) as in Fig. 2.

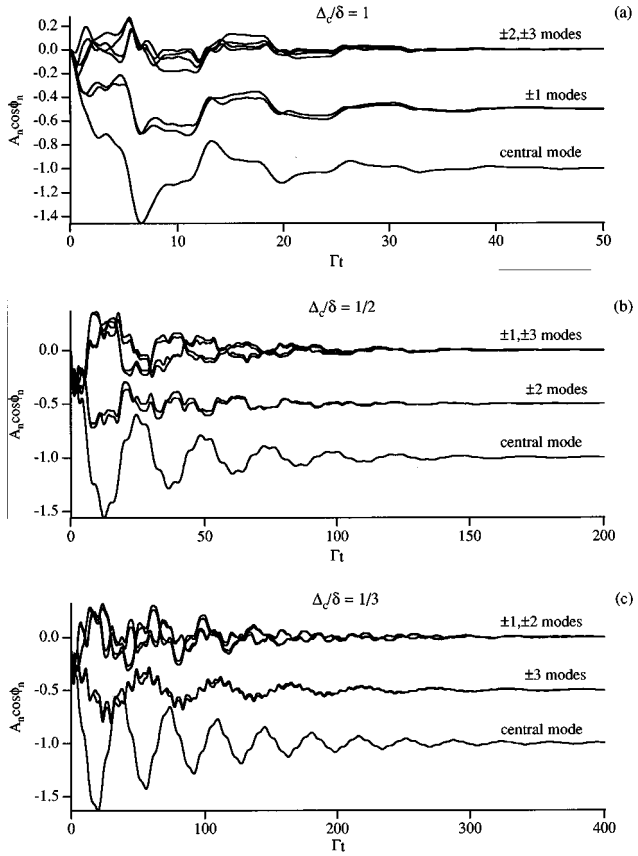

FIG. 5. Seven cavity field modes allowed, with (a) $\Delta_c=\delta$, (b) $\Delta_c=\delta/2$, and (c) $\Delta_c=\delta/3$. In each case, only the real part of the slowly varying cavity field, $A_n\cos\phi_n$, is plotted vs Γt.

which then implies that in this limit $\Omega'=gv\rightarrow-\chi$ and $\Omega''=-gu\rightarrow 0$.

V. GRAPHICAL RESULTS

In all of our numerical experiments, we kept the driving field modulation frequency fixed, so that the driving-field mode spacing was δ. We then varied the number and frequency spacing (Δ_c) of the allowed cavity modes. In all of the following graphs of the cavity field, we plot only the slowly varying part. Writing the cavity field as $\Omega_n=\Omega_{\rm slow}e^{i\Delta_n t}$, we find the slowly varying part can be written as

$$\begin{aligned}\Omega_{\rm slow}&=\Omega_n e^{-i\Delta_n t}\\&=\Omega_n'\cos\Delta_n t+\Omega_n''\sin\Delta_n t+i(\Omega_n''\cos\Delta_n t-\Omega_n'\sin\Delta_n t)\\&=A_n\cos\phi_n+iA_n\sin\phi_n,\end{aligned}\tag{35}$$

where the final line was obtained using Eqs. (21c) and (21d). We plot $A_n\cos\phi_n$ and $A_n\sin\phi_n$ separately in the following figures. We first investigate the case of pure amplitude modulation (setting $c_{\rm fm}=0$), and then show how the results are modified when we generalize the field modulation. The effect of a nonzero cavity damping ($\gamma_c\neq 0$) will be briefly indicated in the final figure.

In each of the figures we set the amplitude of the driving field Rabi frequency equal to $1/T_2=\Gamma$ ($\chi_0=\Gamma$), so that it can be considered to be a relatively strong field, but not so strong as to wash out the atom's natural linewidth. Taking our cue from previous work showing that the best atomic response to a modulated driving field occurs when the modulation frequency is approximately equal to the driving Rabi frequency [18], we set $\delta=\chi_0$.

In Fig. 2 we allow five cavity modes to develop and adjust the cavity so that the cavity field mode spacing equals the driving field mode spacing. The plots show the steady state indicated in Eqs. (22). We see that all the ϕ_n go to zero and the central mode and the ±1 modes develop 180° out of phase with the driving field. The ±2 modes decay away to zero. In Fig. 3 we again allow five cavity modes to develop, but now we set the cavity mode spacing equal to one half the driving mode spacing. This brings the ±2 modes into resonance with the driving field. The ±1 modes and all the ϕ_n decay to zero. Notice from the time scale that the steady state takes much longer to reach than when the ±1 modes were resonant. In Fig. 4 we set the cavity mode spacing equal to two-thirds of the driving field mode spacing ($\Delta_c=\delta/1.5$). In the figure we see that no steady state is ever reached when the cavity mode spacing is not a pure harmonic of the driving field mode spacing (i.e., $\Delta_c\neq\delta/n$).

In Fig. 5 we allow seven cavity modes to develop. Here we show only the $A_n\cos\phi_n$ components of the cavity fields, as once again all the ϕ_n go to zero. As Eqs. (22) indicate, for $\Delta_c=\delta$ the ±1 side modes are resonant with the driving field and become 180° out of phase with it. The ±2 and ±3 modes die away. When the cavity mode spacing is equal to

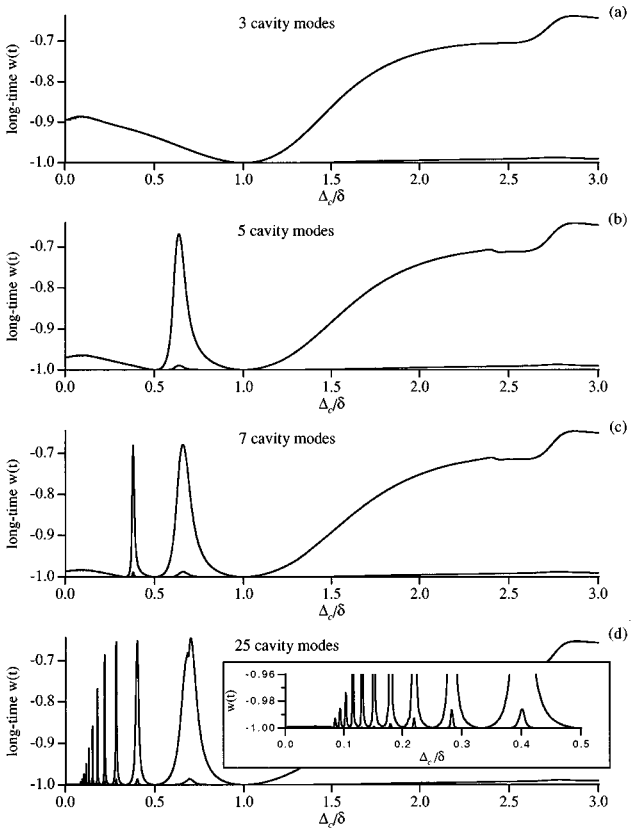

FIG. 6. The maximum and minimum of the atomic inversion w, after $\Gamma t = 400$, vs Δ_c/δ. (a) Three cavity modes allowed. (b) Five cavity modes allowed. (c) Seven cavity modes allowed. (d) Twenty-five cavity modes allowed. The inset is an expansion of the small Δ_c/δ part of the 25-mode graph.

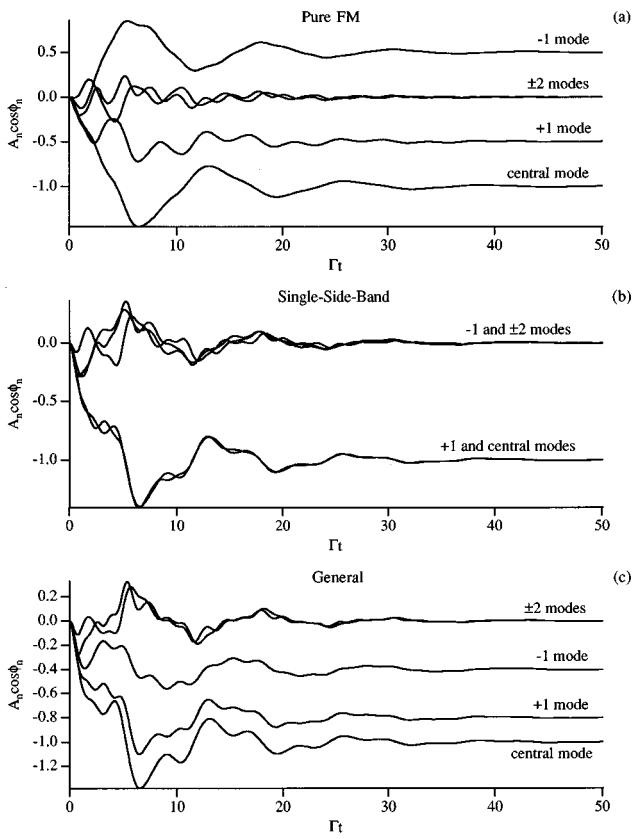

FIG. 7. Five cavity field modes allowed, with $\Delta_c = \delta$. (a) Pure frequency modulation of the driving field ($a_m = 0$). (b) Single-sideband driving field ($a_m = f_m = 1$). (c) Completely general driving field modulation ($a_m = 1.2$, $f_m = 0.4$). In each case, only the real part of the slowly varying cavity field, $A_n \cos\phi_n$, is plotted vs Γt.

the second ($\Delta_c = \delta/2$) or third ($\Delta_c = \delta/3$) harmonic of the driving field, the ± 2 or ± 3 side modes, respectively, move into resonance, leaving the other modes to die away. Notice once again that the steady state is reached after longer and longer periods of time as the resonant modes move away from the central three modes.

In Fig. 6 we plot the maximum and minimum of the atomic inversion w in a long-time limit, as a function of Δ_c/δ. As we have predicted, the inversion remains at -1 in this steady-state limit whenever the cavity field mode spacing is a pure harmonic of the driving field mode spacing.

Figure 7 shows the effects of generalizing the modulation of the driving field. In each of these figures, we allow five cavity modes to develop and only look at the $\Delta_c = \delta$ case, as the effects of going to higher harmonics has already been made clear. Also, we only look at the $A_n \cos\phi_n$ components of the cavity field because in each case all the ϕ_n go to zero, as predicted by Eqs. (22). In (a), the pure frequency-modulated case ($c_{\rm am} = 0$), we see that the central and ± 1 modes develop 180° out of phase with the driving field modes [recall that in frequency modulation, the sidebands are 180° out of phase with each other, hence the $-(\pm 0.5)$ values for the ± 1 modes]. In (b), we show the results when there is only a single sideband ($c_{\rm am} = c_{\rm fm} = 1$). The central and $+1$ modes become 180° out of phase with the driving field and all other modes go to zero. In (c), we let $c_{am} = 1.2$ and $c_{\rm fm} = 0.4$, to represent a completely general modulation of the driving field. As predicted by Eqs. (22), A_{+1} goes to $-1/2(1.2+0.4) = -0.8$ and A_{-1} goes to $-1/2(1.2-0.4) = -0.4$.

Finally, in Fig. 8 we show how the 180° out-of-phase condition of a three-mode cavity field with $\Delta_c = \delta$ in the long-time limit begins to fail as the cavity is made leaky ($\gamma_c > 0$). We only show two nonzero values of γ_c since the trend is obvious.

VI. SUMMARY

In this paper we have provided analytic and numeric results describing the fluorescence of an atom in a cavity being driven by an external time-dependent field. The external field modulation produces a two- or three-mode driving field, so we allow several modes to develop in the cavity.

When the modulation frequency is zero, we obtain the single-mode results of Alsing *et al.* (Ref. [9]). The single-cavity mode becomes 180° out of phase with the driving field mode in steady state. The resultant field at the position of the atom is then zero, and the atom stops fluorescing. When the modulation frequency is made nonzero, the cavity field modes once again develop 180° out of phase with the driving field modes, but only when the cavity field mode

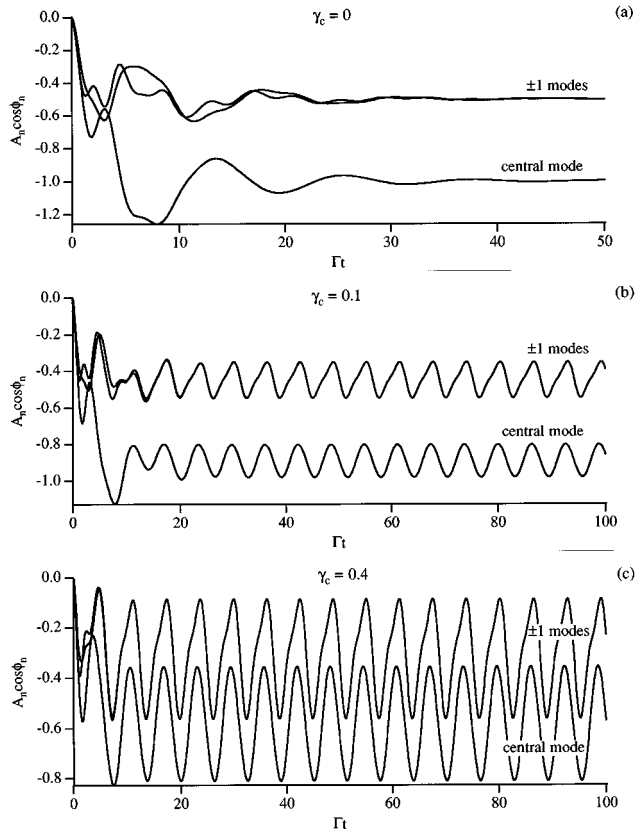

FIG. 8. Three cavity field modes allowed, with $\Delta_c = \delta$. (a) Zero cavity damping ($\gamma_c/\Gamma = 0$). (b) Nonzero cavity damping ($\gamma_c/\Gamma = 0.1$). (c) Even greater cavity losses ($\gamma_c/\Gamma = 0.4$).

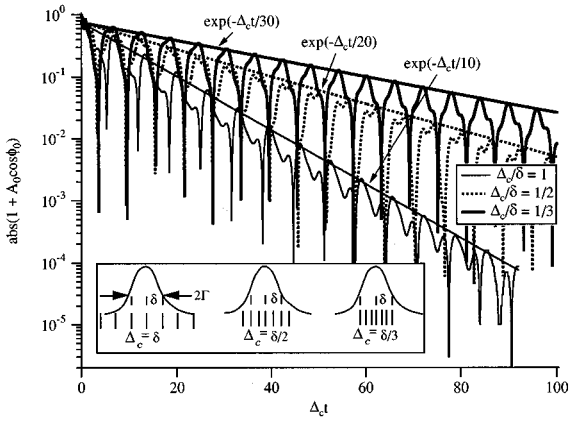

FIG. 9. The absolute value of one plus the real part of the slowly varying central cavity field mode from Fig. 5 (the case in which seven cavity modes are allowed) is plotted on a log scale vs $\Delta_c t$ to show the decay to steady state. (One is added to the mode amplitudes since the steady-state value is a negative one.) The solid thin line has $\Delta_c = \delta$, the dashed line has $\Delta_c = \delta/2$, and the thick solid line has $\Delta_c = \delta/3$. Exponential curves with decay constants of $\Delta_c = \delta/10$, $\Delta_c = \delta/20$, and $\Delta_c = \delta/30$ are also plotted. The inset represents the varying cavity mode spacing Δ_c in relation to the fixed driving mode spacing δ and the atomic linewidth Γ.

spacing is a pure harmonic of the driving field mode spacing. In other words, whenever the central cavity field mode and *any* two of the cavity field side bands match up with the central driving field mode and its two side bands, the atom decouples from the driving field and stops fluorescing. Also, when cavity damping is introduced, the cancellation effect becomes less pronounced.

This cancellation effect is analogous to the field-induced transparency described by Cardimona *et al.* (Refs. [10–12]). In that case, multiple transition paths within a multilevel atom are dressed by an applied field and develop 180° out of phase with each other, thereby adding to zero and causing the atom to decouple from the driving field.

In the system studied in this work, the atom is coupled to the cavity modes and can absorb from and emit into these modes. It can also radiate into free space via spontaneous emission. Therefore, even when cavity damping is absent ($\gamma_c = 0$), the modes of the cavity are damped through their interaction with the atom. In our analysis we find that initially the atom deposits energy into all the cavity modes. However, over time the modes nonresonant with the driving field decay to zero, while the modes resonant with the driving field oscillate to a nonzero value. This continues until, in steady state, the modes resonant with the driving field are equal and opposite to the driving field, at which point the atom decouples from the field. From Fig. 5 we see that the time necessary to reach this steady state increases as we decrease the ratio of Δ_c/δ. For fixed δ, this means that the steady state is pushed farther off when the cavity mode spacing Δ_c is reduced. Reducing Δ_c increases the number of nonresonant modes within the radiative atomic linewidth Γ (see the inset in Fig. 9). If we plot the cavity field modes as a function of the cavity mode time scale $\Delta_c t$, we find that they decay at a rate proportional to Δ_c/n when $\Delta_c = \delta/n$. The physical reason behind this is that when $\Delta_c = \delta$, there is only one set of sidebands within the atomic linewidth (since $\delta = \Gamma$). The other sidebands outside the atomic response linewidth interact only very weakly with the atom. When $\Delta_c = \delta/n$, n sets of cavity field sidebands fall within the atomic linewidth, feeding off each other and supporting each other in a non-steady-state for a longer period of time. In Fig. 9 we demonstrate the above explanation by plotting the absolute value of the real part of the central cavity mode for the seven-mode case versus $\Delta_c t$ for $\Delta_c = \delta/1$, $\Delta_c = \delta/2$, and $\Delta_c = \delta/3$, as well as three exponential curves with decay constants equal to $\Delta_c/10$, $\Delta_c/20$, and $\Delta_c/30$. The semilogarithmic scale produces straight lines for the exponential curves.

We also showed how the multimode equations reduce, in the infinite cavity limit, to the neoclassical equations of Stroud and Jaynes (Ref. [17]). In this limit, we reproduce the field-cancellation effect when the absorption (αa_0) is greater than 1.

When we allowed modulation other than pure amplitude modulation, the cancellation effect persisted. Since any arbitrary three-mode field can be constructed with combinations of amplitude modulation and frequency modulation, and since the above results can be easily extended to more than three-mode driving fields, the field cancellation effect described in this paper should apply to any general time-dependent field driving a two-level atom in a multimode cavity.

[1] E. T. Jaynes and F. W. Cummings, Proc. IEEE **51**, 89 (1963).
[2] J. Opt. Soc. Am. B **6**, 2020 (1989), special issue on laser cooling and trapping of atoms.
[3] H. J. Carmichael, Phys. Rev. Lett. **55**, 2790 (1985).
[4] P. R. Price and H. J. Carmichael, IEEE J. Quantum Electron. **24**, 1351 (1988).
[5] C. M. Savage and H. J. Carmichael, IEEE J. Quantum Electron. **24**, 1495 (1988).
[6] P. R. Price and H. J. Carmichael, J. Opt. Soc. Am. B **5**, 1661 (1988).
[7] H. J. Carmichael, R. J. Brecha, and P. R. Price, Opt. Commun. **82**, 73 (1991).
[8] P. M. Alsing and H. J. Carmichael, Quant. Opt. **3**, 13 (1991).
[9] P. M. Alsing, D. A. Cardimona, and H. J. Carmichael, Phys. Rev. A **45**, 1793 (1992).
[10] D. A. Cardimona, M. G. Raymer, and C. R. Stroud, Jr., J. Phys. B **15**, 55 (1982).
[11] D. A. Cardimona, M. P. Sharma, and M. A. Ortega, J. Phys. B **22**, 4029 (1989).
[12] D. A. Cardimona, Phys. Rev. A **41**, 5016 (1990).
[13] S. E. Harris, J. E. Field, and A. Imamoglu, Phys. Rev. Lett. **64**, 1107 (1990).
[14] A. Imamoglu, J. E. Field, and S. E. Harris, Phys. Rev. Lett. **66**, 1154 (1991).
[15] K.-J. Boller, A. Imamoglu, and S. E. Harris, Phys. Rev. Lett. **20**, 2593 (1991); J. Gea-Banacloche, Y. Li, S. Jin, and M. Xiao, Phys. Rev. A **51**, 576 (1995); D. J. Fulton, S. Shepherd, R. R. Moseley, B. D. Sinclair, and M. H. Dunn, *ibid.* **52**, 2302 (1995).
[16] Hwei P. Hsu, *Fourier Analysis* (Simon & Schuster; New York, 1970), pp. 236–239.
[17] C. R. Stroud, Jr. and E. T. Jaynes, Phys. Rev. A **1**, 106 (1970).
[18] L. W. Hillman, J. Krasinski, K. Koch, and C. R. Stroud, Jr., J. Opt. Soc. Am. B **2**, 211 (1985); K. Koch, B. J. Oliver, S. H. Chakmakjian, and C. R. Stroud, Jr., *ibid.* **6**, 58 (1989).